Inorg. Chem. **2005**, *44*, 2553–2559

Synthesis, Structure, and Large Optical Limiting Effect of the First Coordination Polymeric Cluster Based on an {I@[AgI(inh)]$_6$} Hexagram Block

Yunyin Niu,[†] Yinglin Song,[‡] Hongwei Hou,*[,†] and Yu Zhu[†]

Department of Chemistry, Zhengzhou University, Henan 450052, P.R. China, and Department of Applied Physics, Harbin Institute of Technology, Heilongjiang 150001, P.R. China

Received September 15, 2004

In this paper, treatment of *N*-(isonicotinoyl)-*N*′-nicotinoylhydrazine (inh) and AgI with excess KI afforded a unique coordination polymeric cluster {[AgI(inh)]$_6$(KI)}$_n$ (**1**) with the hexagram cluster units centered by μ_6-I. In the polymer these hexagram units are parallel to the *ab* plane and are linked by separated K^+ centers through inh. Polymer **1** represents the first example of coinstantaneous cation–anion-induced supramolecular self-assembly with nanoscale inner cavities. The polymer's third-order nonlinear optical (NLO) properties were determined by the *Z*-scan technique in DMF solution. The results show that the polymer has strong third-order optical nonlinearities. The nonlinear absorptive index a_2 and refractive index n_2 are calculated to be 1.044×10^{-9} mW^{-1} and 2.827×10^{-11} esu, respectively. The values are comparable to those of the reported cluster polymers. The optical limiting experiments show that the present cluster exhibits a large optical limiting capacity. The value of the limiting threshold was measured as 0.53 J cm^{-2} from the optical limiting experimental data. This value is three times better than 1.6 J cm^{-2} of C_{60}. This paper also gives a summary and comparison on the optical limiting properties of oligomeric and polymeric clusters.

Introduction

The design and construction of organic/inorganic supramolecular architectures with inner cavities is a rapidly developing area that has offered promising perspective toward developing new functional materials;[1] among which optical limiting materials are substances whose transmission is high when they are illuminated by low-intensity light but low when exposed to intense laser radiation. Because of their potential applications in the protection of optical sensors from high-intensity laser beams, the search for better optical limiting materials has become increasingly intensive. The most frequently reported materials are fullerenes (C_{60})[2] and phthalocyanine complexes,[3] which are generally regarded as the best compounds for optical limiting. Recently, large nonlinear optical effects have also been observed in inorganic clusters and their polymers.[4] Previous studies showed that most planar clusters (Chart 1) with higher symmetry have superior optical limiting properties.[4b] The higher symmetry may decrease the probability of ground-state electronic transitions and give a smaller absorption cross section σ_g and a larger σ_e/σ_g ($K\alpha$) ratio. In addition, the assembly of monomeric cluster units into a polymer also brought enhancement of optical limiting effect.[4c] Among the structure/NLO property correlation of clusters and polymers, the heavy atom effect also plays an important role.[4d] All the silver-containing clusters have lower thresholds than those of the copper-containing homologues. The W-containing clusters

* Author to whom correspondence should be addressed. E-mail: houhongw@zzu.edu.cn. Tel and fax: +86-371-7761744.
[†] Zhengzhou University.
[‡] Harbin Institute of Technology.

(1) (a) Fujita, M.; Kwon, Y. J.; Washizu, S.; Ogura, K. *J. Am. Chem. Soc.* **1994**, *116*, 1151. (b) Hong, M. C.; Zhao, Y. J.; Su, W. P.; Cao, R.; Fujita, M.; Zhou, Z. Y.; Chan, A. S. C. *Angew. Chem., Int. Ed.* **2000**, *39*, 2468.
(2) (a) Tutt, L. W.; Kost, A. *Nature* **1992**, *356*, 224. (b) McLean, R. L.; Sutherland, M. C.; Brant, D. M.; Brandelik, P. A.; Pottenger, T. *Opt. Lett.* **1993**, *18*, 858.
(3) (a) Perry, J. W.; Mansour, K.; Marder, S. R.; Perry, K. J.; Alvarez, J. D.; Choong, I. *Opt. Lett.* **1994**, *19*, 625. (b) Perry, J. W.; Mansour, K.; Lee, I.-Y. S.; Wu, X.-L.; Bedworth, P. V.; Chen, C. T.; Ng, D.; Marder, S. R.; Miles, P.; Wada, T.; Tian, M.; Sasabe, H. *Science* **1996**, *273*, 1533.
(4) (a) Shi, S.; Ji, W.; Tang, S. H.; Lang, J. P.; Xin, X. Q. *J. Am. Chem. Soc.* **1994**, *116*, 3615. (b) Zhang, C.; Song, Y. L.; Fung, B. M.; Xue, Z. L.; Xin, X. Q. *Chem. Commun.* **2001**, 843. (c) Zhang, Q. F.; Niu, Y. Y.; Leung, W. H.; Song, Y. L.; WilliamsI. D.; Xin, X. Q. *Chem. Commun*. **2001**, 1126. (d) Niu, Y. Y.; Zheng, H. G.; Hou, H. W.; Xin, X. Q. *Coord. Chem. Rev*. **2004**, *248*, 169.

10.1021/ic0487023 CCC: $30.25
Published on Web 03/01/2005

Chart 1. Clusters with a "Planar" Structure

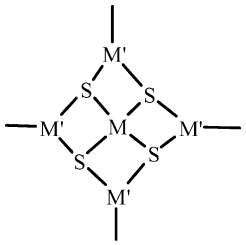

seem always able to outperform their corresponding Mo-containing counterparts in OL performance. This very fact strongly implies that heavy atom-containing polymeric clusters with high symmetry may be designed and synthesized to obtain predictable and controllable NLO properties.

In addition, the peripheral ligands also have an impact on the NLO properties; cluster $[NEt_4]_2[WSe_4(CuS_2CNMe_2)_4]$ with planar structure has a higher limiting threshold (1.1 J cm^{-2}).[5] The result may be attributed to the electronic effect of the peripheral ligands: the π-conjugating ligand $R_2NCS_2^-$ conjugates the skeleton and cluster core moiety, resulting in delocalization of electron density among the metal atoms. It is well-known a successful organic ligand may store readable information interactive with metal ions including steric hindrance, rigidity, length, binding sites, and especially symmetry.[6] However, sometimes asymmetrical ligands can also give unique architectures.[7] On the basis of these experimental facts, we reasoned that an excellent multifunctional ligand might combine the above advantages via coordination with heavy atom-containing metalates such as AgI and lead to molecule with unique structure and properties. To gain an explicit structure/NLO property correlation of clusters and polymers, we extend our study to iodometalate polymeric clusters. Here we report the first anion−cation-induced coordination polymeric cluster $\{[AgI(inh)]_6(KI)\}_n$, which was obtained from silver iodide reacting with the asymmetric bis(pyridine) ligand *N*-(isonicotinoyl)-*N*′-nicotinoylhydrazine (inh), and find that it shows large optical limiting properties.

Experimental Section

General Details. All chemicals were of reagent-grade quality and were obtained from commercial sources and used without further purification. ^{1}H NMR spectra were recorded on a Bruker DPX-400 spectrometer. C, H, and N analyses were carried out on a Carlo-Erba 1106 elemental analyzer. IR data were recorded on a Bruker TENSOR 27 spectrophotometer with KBr pellets in the 400−4000 cm^{-1} region.

The molecular weights and molecular weight distributions of the polymer were determined at 40 °C with gel permeation chromatography (Waters Associates model HPLC/GPC 515 liquid chromatograph, equipped with a refractive index detector and μ-Styragel columns and calibrated with standard polystyrene), using DMF as the eluent and a flow rate of 1.0 mL min^{-1}.

Preparation of the Ligand *N*-(Isonicotinoyl)-*N*′-Nicotinoylhydrazine (inh). The ligand inh was prepared by the acylation of isonicotinoyl chloride with nicotinoylhydrazine in anhydrous pyridine. Isonicotinic acid (5.95 g, 10 mmol) and 20 mL of thionyl chloride were mixed and refluxed for 10 h with exclusion of moisture. Then the excess of thionyl chloride was removed and 20 mL anhydrous pyridine was added to dissolve. This solution was dropped slowly into an anhydrous pyridine solution of nicotinoylhydrazine (1.37 g, 10 mmol) on an ice−salt bath. The mixture was heated to 80 °C, and the resulting deep red solution was inspected by TLG until the reaction finished. Upon removal of the solvent the oil was treated with a saturated $NaCO_3$ solution to pH = 7 to give light-yellow precipitates (yield: 1.8 g, 75%), which were collected by filtration and washed with water. IR (KBr pellet)/cm^{-1}: 3406 b, 3208 b, 3000 b, 1689 s, 1653 vs, 1598 s, 1532 s, 1474 m, 1418 m, 1300 vs, 1122 m, 1033 m, 888 w, 838 w, 696 s, 681 m, 560 w. ^{1}H NMR (400 MHz, DMSO-d_6): δ 10.9510.87 (s, H_3 + H_4), 9.08 (d, H_5), 8.80 (t, H_2 + $H_{2'}$ + H_8), 8.27, (d, H_6), 7.83 (t, H_1 + $H_{1'}$), 7.60 (d−d, H_7).

Preparation of Clusteric Polymer $[(AgIC_{12}H_{10}N_4O_2)_6(KI)]_n$ (1). A solution of inh (0.0242 g, 0.1 mmol) in methanol (4 cm^3) was added to a solution of AgI (0.0235 g, 0.1 mmol) with KI (0.0996 g, 0.6 mmol) in THF−H_2O (6 cm^3 with volume ratio 10:1), and the resulting solution was evaporated in the dark to give the product as pink crystals in ca. 20% yield after 1 month. IR (KBr pellet)/cm^{-1}: 3207 vs, 3038 w, 1689 s, 1653 vs, 1597 m, 1531 s, 1474 m, 1417 m, 1300 s, 1219 w, 1190 w, 1122 w, 1033 w, 888 m, 838 w, 696 s, 560 m, 420 w. ^{1}H NMR (400 MHz, DMSO-d_6): δ 10.92 10.85(s, H_3 + H_4), 9.08 (s, H_5), 8.80 (s, H_2 + $H_{2'}$ + H_8), 8.27 (d, H_6), 7.83 (d, H_1 + $H_{1'}$), 7.74 (d−d, H_7). Found: C, 28.65; H, 2.92; N, 11.26. Calcd for $C_{72}H_{60}Ag_6I_7KN_{24}O_{12}$: C, 28.60; H, 2.30; N, 11.12.

X-ray Crystallography. Crystals of **1** were directly obtained from the reaction mixture. A suitable single crystal (0.20 × 0.20 × 0.20 mm) was selected and mounted on a Rigaku RAXIS-IV image plate area detector for study using graphite-monochromated Mo Kα (λ = 0.710 73 Å) radiation at 291(2) K. The unit cell parameters were determined from the reflections collected on oscillation frames and were then refined. The data were corrected for Lorentz and polarization effects. The structures were solved by direct methods with SHELXS-97[8] and subsequent Fourier-difference synthesis and refined by the full-matrix least-squares method on F^2 with SHELXL-97.[9] All non-hydrogen atoms were refined anisotropically, and hydrogen atoms were placed at calculated positions and refined as riding atoms with isotropic displacement parameters. Crystal data and structure refinement details for the compound are given in Table 1. Selected bond lengths and angles are given in Table 2.

Nonlinear Optical Measurements. The optical measurements were performed with linearly polarized 7-ns pulses at 532 nm generated from a frequency-doubled Q-switched Nd:YAG laser; this wavelength is of paramount practical importance in the field of optical limiting as well as design and fabrication of the resonance cavities of lasers. The spacial profiles of the pulses were nearly Gussian after a spatial filter was employed. A DMF solution of

(5) Zhang, Q. F.; Bao, M. T.; Hong, M. C.; Cao, R.; Song, Y. L.; Xin, X. Q. *J. Chem. Soc., Dalton Trans.* **2000**, 605.
(6) Lehn, J. M. *Supramolecular Chemistry: Concepts and Perspectives*; VCH: Weinheim, Germany, 1995.
(7) (a) Bretonniere, Y.; Mazzanti, M.; Pecaut, J.; Olmstead, M. *J. Am. Chem. Soc.* **2002**, *124*, 9012. (b) Qin, Z. Q.; Jennings, M. L. C.; Puddephatt, R. J. *Chem. Commun.* **2001**, 2676. (c) Tong, M. L.; Li, L. J.; Mochizuki, K. H. C.; Chen, X. M.; Li, Y.; Kitagawa, S. *Chem. Commun.* **2003**, 428. (d) Adams, H.; Clunas, S.; Fenton, D. E. *Chem. Commun.* **2002**, 418. (e) Lee, I. S.; Shin, D. M.; Chung, Y. K. *Chem.—Eur. J.* **2004**, *10*, 3158.
(8) Sheldrick, G. M. *Acta Crystallogr., Sect. A* **1990**, *46*, 467.
(9) Sheldrick, G. M. *SHELXL-97, Program for the Refinement of Crystal Structures*; University of Göttingen: Göttingen, Germany, 1997.

Table 1. Crystal Data and Data Collection and Structure Refinement Parameters for **1**

formula	$C_{72}H_{60}Ag_6I_7KN_{24}O_{12}$
fw	3028.06
cryst system	rhombohedral
space group	$R\bar{3}$
a/Å	20.457(3)
b/Å	20.457(3)
c/Å	18.516(4)
α/deg	90.00
β/deg	90.00
γ/deg	120.00
V/Å^3	6710.6(19)
Z	3
ρ_{calc}/Mg m^{-3}	2.248
μ/mm^{-1}	3.820
F(000)	4284
cryst size/mm	0.20 × 0.20 × 0.20
reflcns measd	6447
reflcns used (R_{int})	2502
temp/K	291(2)
λ(Mo Kα)/Å	0.710 73
$2\theta_{max}$/deg	50.00
R_{int}	0.0295
data/restraints/params	2502/0/194
GOF on F^2	1.058
final R1,[a] wR2[b]	0.0342, 0.0641
R indices (all data)	0.0588, 0.0683
largest peak and hole/e Å^{-3}	0.978, −1.299

[a] $R1 = \Sigma||F_o| - |F_c||/\Sigma|F_o|$. [b] $wR2 = [\Sigma w(|F_o^2| - |F_c^2|)^2/\Sigma w|F_o^2|^2]^{1/2}$; $w = 1/[\sigma^2(F_o)^2 + 0.0297P^2 + 27.5680P]$, where $P = (F_o^2 + 2F_c^2)/3$.

Table 2. Selected Bond Lengths (Å) and Bond Angles (deg) for Polymer **1**[a]

Ag(1)−I(2)	2.7762(7)	Ag(1)−I(1)	3.0906(7)
Ag(1)−I(2)$^{\#1}$	2.7414(7)	I(1)−Ag(1)$^{\#2}$	3.0906(7)
I(1)−Ag(1)$^{\#1}$	3.0906(7)	I(1)−Ag(1)$^{\#3}$	3.0906(7)
I(1)−Ag(1)$^{\#5}$	3.0906(7)	I(1)−Ag(1)$^{\#4}$	3.0906(7)
I(2)−Ag(1)$^{\#2}$	2.7414(7)	Ag(1)−N(1)	2.372(4)
Ag(1)−Ag(1)$^{\#1}$	3.2322(8)	O(1)−K(1)	2.666(4)
I(2)$^{\#1}$−Ag(1)−I(2)	129.50(2)	I(2)$^{\#1}$−Ag(1)−I(1)	109.219(19)
I(2)−Ag(1)−I(1)	108.293(19)	I(2)$^{\#1}$−Ag(1)−Ag(1)$^{\#1}$	54.641(19)
I(2)$^{\#1}$−Ag(1)−Ag(1)$^{\#2}$	129.19(3)	I(1)−Ag(1)−Ag(1)$^{\#1}$	58.472(3)
I(2)−Ag(1)−Ag(1)$^{\#1}$	162.11(2)	I(2)−Ag(1)−Ag(1)$^{\#2}$	53.643(18)
I(1)−Ag(1)−Ag(1)$^{\#2}$	58.472(3)	Ag(1)$^{\#1}$−I(1)−Ag(1)$^{\#3}$	180.00(2)
Ag(1)$^{\#1}$−I(1)−Ag(1)$^{\#4}$	63.056(5)	Ag(1)$^{\#3}$−I(1)−Ag(1)$^{\#4}$	116.944(5)
Ag(1)$^{\#1}$−I(1)−Ag(1)$^{\#5}$	116.944(5)	Ag(1)$^{\#3}$−I(1)−Ag(1)$^{\#5}$	63.056(5)
Ag(1)$^{\#4}$−I(1)−Ag(1)$^{\#5}$	63.056(5)	Ag(1)$^{\#1}$−I(1)−Ag(1)$^{\#2}$	116.944(5)
Ag(1)$^{\#5}$−I(1)−Ag(1)$^{\#2}$	116.944(5)	Ag(1)$^{\#4}$−I(1)−Ag(1)$^{\#2}$	180.00(2)
Ag(1)$^{\#4}$−I(1)−Ag(1)	116.944(5)	Ag(1)$^{\#5}$−I(1)−Ag(1)	180.00(2)
Ag(1)$^{\#3}$−I(1)−Ag(1)$^{\#2}$	63.056(5)	Ag(1)$^{\#2}$−I(2)−Ag(1)	71.72(2)
Ag(1)$^{\#1}$−I(1)−Ag(1)	63.056(5)	Ag(1)$^{\#3}$−I(1)−Ag(1)	116.944(5)
Ag(1)$^{\#2}$−I(1)−Ag(1)	63.056(5)	N(1)−Ag(1)−I(2)	100.52(11)
N(1)−Ag(1)−I(2)$^{\#1}$	109.25(11)	N(1)−Ag(1)−I(1)	94.00(11)
N(1)−Ag(1)−Ag(1)$^{\#2}$	120.12(11)	N(1)−Ag(1)−Ag(1)$^{\#1}$	92.83(11)
O(1)$^{\#6}$−K(1)−O(1)$^{\#7}$	84.82(11)	C(6)−O(1)−K(1)	151.3(4)
O(1)$^{\#6}$−K(1)−O(1)$^{\#3}$	180.0	O(1)$^{\#6}$−K(1)−O(1)	95.18(11)
O(1)$^{\#3}$−K(1)−O(1)	84.82(11)	O(1)$^{\#3}$−K(1)−O(1)$^{\#7}$	95.18(11)
O(1)−K(1)−O(1)$^{\#7}$	180.0	O(1)$^{\#6}$−K(1)−O(1)$^{\#8}$	84.82(11)
O(1)$^{\#3}$−K(1)−O(1)$^{\#8}$	95.18(11)	O(1)−K(1)−O(1)$^{\#8}$	95.18(11)
O(1)$^{\#7}$−K(1)−O(1)$^{\#8}$	84.82(11)	O(1)$^{\#6}$−K(1)−O(1)$^{\#4}$	95.18(11)
O(1)$^{\#3}$−K(1)−O(1)$^{\#4}$	84.82(11)	O(1)−K(1)−O(1)$^{\#4}$	84.82(11)
O(1)$^{\#7}$−K(1)−O(1)$^{\#4}$	95.18(11)	O(1)$^{\#8}$−K(1)−O(1)$^{\#4}$	180.0

[a] Symmetry codes for polymer **1**: (#1) $y, -x + y, -z$; (#2) $x - y, x, -z$; (#3) $-y, x - y, z$; (#4) $-x + y, -x, z$; (#5) $-x, -y, -z$; (#6) $y, -x + y, -z + 1$; (#7) $-x, -y, -z + 1$; (#8) $x - y, x, -z + 1$.

compound **1** was placed in a 1-mm-thick quartz cell for optical limiting measurements. The crystal samples were stable toward oxygen, moisture, and laser light. The laser beam was focused with a 25-cm focal-length focusing mirror. The radius of the beam circumference was measured to be 30 ± 5 μm (half-width at 1/e^2 maximum in irradiance). The incident and transmitted pulse energy were measured simultaneously by two energy detectors (Laser Precision Rjp-735) which were linked to a computer by an IEEE interface.[10,11] The interval between the laser pulses was chosen to be ∼5 s for operational convenience and controlled by the computer. The NLO properties of compound **1** were manifested by moving the sample along the axis of the incident laser beam (*Z*-direction) with respect to the focal point instead of being positioned at its focal point, and an identical setup was adopted in the experiments to measure the *Z*-scan data.

Results and Discussion

Preparation of the Complex. Although many heterometallic polymeric clusters have been synthesized, many aspects such as the synthesis, reaction chemistry, and properties of homometallic polymers are only poorly explored. Our interest in this area will mainly focus on the exploration of new aggregate iodometalate clusters with desired NLO properties and the development of new synthetic routes for polymeric clusters via the formation of I_3^- complex anion. It is well-known that the solubility of insoluble salts is crucial for the synthesis of the related complexes. Several strategies have been employed to circumvent this practical problem. In addition to the routine method of seeking and utilization of appropriate solvents, the formation of I_3^- complex may also increase greatly the solubility of univalent metal iodides via the addition of excesses KI or NaI. The active intermediate I_3^- complex is a good iodine origin for cluster construction, and the self-assembly reaction of it with ligands is an effective route for preparation of novel polymeric complexes containing iodine cluster. With this method we had already obtained a 2D "open" polymer $[AgI(bpe)]_n$ (bpe =1,2-bis-(4-pyridyl)ethane) with the "staircase" cluster units connected by regular bpe bridges.[12a] This procedure can also produce the 2D interpenetrating polymeric cluster $[Cu(4,4'\text{-bipyridine})I]_n$ reported by others.[12b,c]

Most symmetrical multifunctional ligands were designed and employed to fabricate coordination polymers; the asymmetrical ligands were seldom used in the absence of the symmetrical center. However sometimes the multicoordinating sites in the ligands can make up the disadvantages. We obtained the novel title polymer in this reaction system; this may be due to the structural characteristics of inh ligand. In the inh ligand although the nicontinoyl N site was left unused, the nicontinoyl carbonyl O's coordination constructs the K^+ octahedral configuration and the final polymer catena. The complex is stable in the air. It is not soluble in common organic solvents, such as MeOH, EtOH, MeCN, and THF, but just soluble in highly polar solvents DMSO or DMF. Single crystals suitable for X-ray crystallography for the compound were collected by slow evaporation of the THF/H_2O solutions in the dark.

Description of Crystal Structure. An X-ray diffraction study confirmed the structure to be a catena polymer with

(10) Sheik-bahae, M.; Said, A. A.; Wei, T. H.; Hangan, D. J.; Van Stryland, E. W. *IEEE J. Quantum Electron.* **1990**, *26*, 760.
(11) Sheik-bahae, M.; Said, A. A.; Van Stryland, E. W. *Opt. Lett.* **1989**, *14*, 955.
(12) (a) Niu Y. Y., Hou, H. W. Zhu, Y. *J. Cluster Sci.* **2003**, *4*, 483. (b) Batten, S. R.; Jeffery, J. C.; Ward, M. D. *Inorg. Chim. Acta* **1999**, *292*, 231. (c) Blake, A. J.; Brooks, N. R.; Champness, N. R.; Cooke, P. A.; Crew, M.; Deveson, A. M.; Hanton, L. R.; Hubberstey, P.; Fenske, D.; Schröder, M. *Cryst. Eng.* **1999**, *2*, 181.

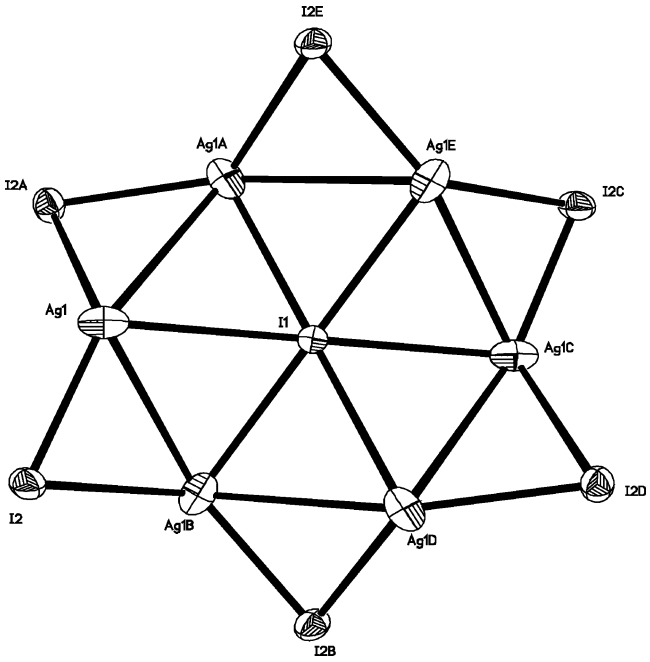

Figure 1. Structure of the $[I@Ag_6I_6]^-$ hexagram cluster unit in **1** with the atom-numbering scheme.

Scheme 1. Assembly Procedure of Cluster **1**

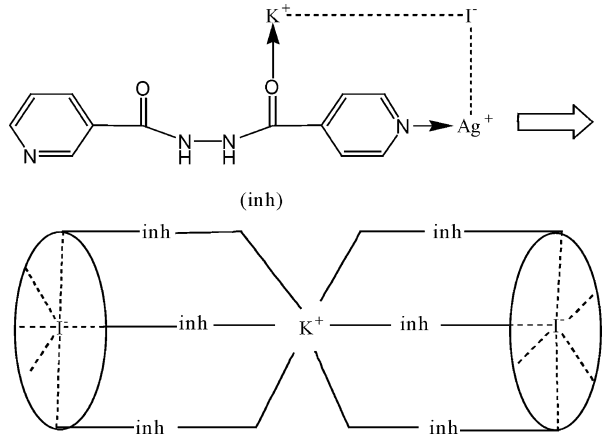

alternate I^--centered and K^+-centered coordination units (Scheme 1).

Each silver atom is coordinated by one N atom from an inh and three I atoms in a distorted tetrahedral fashion [I−Ag−I angles in the range of 108.219(2)−129.50(2)° and I−Ag−N angles in the range of 94.00(1)−109.25(1)°]. The six silver atoms in each $[Ag_6I_7]^-$ core are in a chairlike arrangement with Ag−Ag−Ag angles of 109.180(16)° (Figure 1). The adjacent Ag−Ag distance (3.2322(8) Å) is well below the summed van der Waals contact distance (3.44 Å).[13] This kind of arrangement forms a hexagram motif together with six peripheral μ-I atoms. The seventh iodide atom, μ_6-I1, is located at the center of the hexagram and σ-bonded to six Ag atoms at a distance of 3.09 Å in the *ab* plane. Although a series of monomeric Ag_6 octahedron clusters[14] and polymeric Ag_6 octahedron units centered by anion such as μ_6-C_2^{2-}, μ_6-F, μ_3-F, and μ_3-CF_3SO_3[15] have been reported, this $[Ag_6I_6]$ hexagram cluster centered by μ_6-I^- is of unknown precedence. These hexagrams are parallel to the *ab* plane and are linked by separated K^+ centers through inh.

Each inh links one silver atom through its isonicontinoyl N atom and ligates the K^+ atom through the nicontinoyl carbonyl O atom with Ag−N distance of 2.372(4) Å and K−O distance of 2.666(4) Å. The C═N (1.330(7)−1.347(7) Å) and N−N bond distances (1.396(6) Å) are consistent with those in related compounds.[16] Among the six inh bonded to the resulting $\{[I@Ag_6][I(inh)]_6\}$ unit, three inh coordinate from the left and three from the right (Figure 2). A similar coordinate mode also produces the K^+ complex octahedron: each potassium atom bonded to three oxygen atoms from the left inh and three oxygen atoms from the right inh at a distance of 2.666(4) Å. Although the potassium cation center shows no ionic involvement with the μ_6-iodide center and has $K^+\cdots I^-$ distances of 9.258 Å [ionic distance K−I average 3.76(1) Å],[17] the charge balance is still achieved by the array of pairs of K^+ and I^- along polymeric *c*-axis direction. So the central countercharge $K^+\cdots I^-$ ion pairs appear to play an important directed role.

An alternate viewpoint to see **1** is that it is a bamboo-shaped polymer with a largest inner diameter of about 1 nm [9.518−9.917 Å, defined as the furthest I−I or O−O distance parallel to the *ab* plane]. A particularly salient feature of the polymeric structure is the charge-balanced $K^+\cdots I^-$ ion pairs trapped within the cavity of the molecule, which serve as the nut⋯bolt of the tubelike combination (Figure 3). It is unlikely that an empty "tube" is preformed for the encapsulation of the ion pairs; instead, the formation of the polymeric cluster can be best described as a $K^+\cdots I^-$ ion pair-induced self-assembly of the Ag^+ ions and inh ligands. In addition, although there are many examples for self-assembly induced or controlled by an anion (such as Cl^-, $SO_3CF_3^-$)[18] or cation (such as $[\{Ag\}^{II}(\{tmc\})(\{BF\}_4)]_\infty^+$),[19] complex **1** represents a first product of assembly induced by coexistent cation−anion pairs.

Nonlinear Optical Properties. The study on coordination polymers is greatly focused on novel structures and properties. Recently we found that many coordination polymers exhibit interesting third-order nonlinearities in DMF solution.

(13) Bondi, A. *J. Phys. Chem*. **1964**, *68*, 441.

(14) (a) Yam, V. W. W.; Cheng, E. C. C.; Zhu, N. Y. *New J. Chem*. **2002**, *26*, 279. (b) Dietrich, H.; Storck, W.; Manecke, G. *J. Chem. Soc., Chem. Commun*. **1982**, 1036. (c) Briant, C. E.; Smith, R. G.; Mingos, D. M. P. *J. Chem. Soc., Chem. Commun.* **1984**, *9*, 586. (d) Liu, C. W.; Shang, I. J.; Wang, J. C.; Keng, T. C. *Chem. Commun.* **1999**, 995.

(15) (a) Guo, G. C.; Wang, Q. G.; Zhou, G. D.; Mak, T. C. W. *Chem. Commun*. **1998**, 339. (b) Wang, Q. M.; Mak, T. C. W. *J. Am. Chem. Soc*. **2000**, *122*, 7608. (c) Wang, Q. M.; Mak, T. C. W. *Chem. Commun*. **2000**, 1435.

(16) (a) Bu, X. H.; Liu, H.; Du, M.; Zhang, L.; Guo, Y. M.; Shionoya, M.; Ribas, J. *Inorg. Chem.* **2002**, *41*, 1855. (b) Matthews, C. J.; Avery, K.; Xu, Z. Q.; Thompson, L. K.; Zhao, L.; Miller, D. O.; Biradha, K.; Poirier, K.; Zaworotko, M. J.; Wilson, C.; Goeta, A. E.; Howard, J. A. K. *Inorg. Chem.* **1999**, *38*, 5266.

(17) Rath, N. P.; Holt, E. M. *J. Chem. Soc., Chem. Commun*. **1985**, 665.

(18) (a) Withersby, M. A.; Blake, A. J.; Champness, N. R.; Hubberstey, P.; Li, W. S.; Schroder, M. *Angew. Chem., Int. Ed. Engl.* **1997**, *36*, 2327. (b) Wang, R. Y.; Zheng, Z. P.; Jin T. Z.; Staples, R. J. *Angew. Chem., Int. Ed.* **1998**, *38*, 1813. (c) James, S. L.; Mingos, D. M. P.; White, A. J. P.; Williams, D. J. *Chem. Commun.* **1998**, 2323.

(19) Wang, Q. M.; Mak, T. C. W. *Chem. Commun.* **2001**, 807.

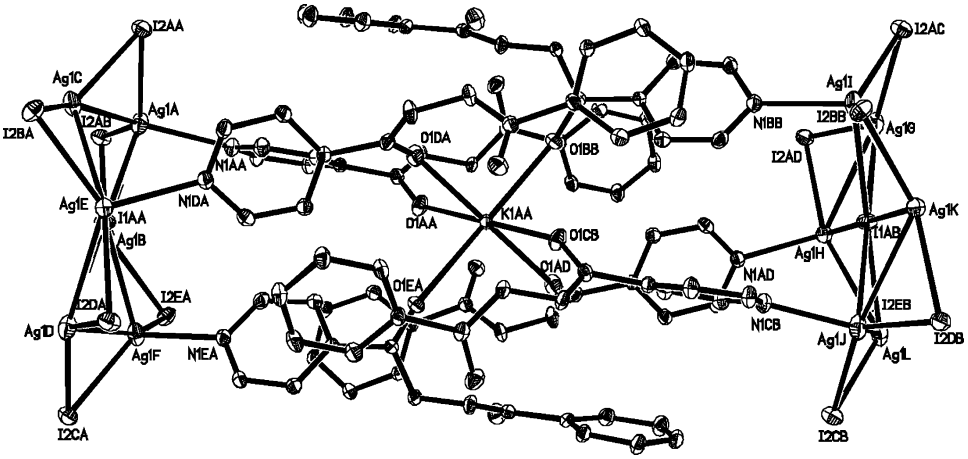

Figure 2. Crystal structure of the basic {[I@Ag$_6$][I(inh)]$_6$} unit with thermal ellipsoids at 30% probability. The H atoms are omitted for clarity.

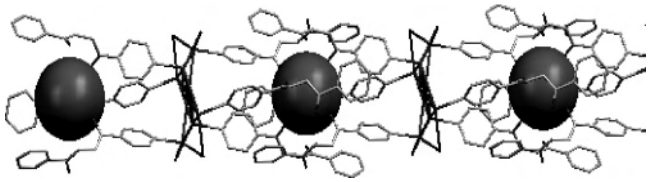

Figure 3. View of the KI-induced assembly in **1**. The large spheres represent K atoms.

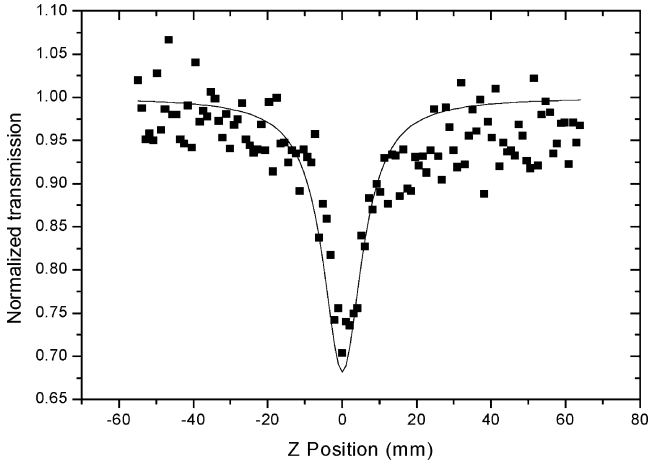

Figure 4. *Z*-scan data for **1** in 1.0 × 10^{-5} mol dm^{-3} DMF solution, obtained under an open aperture configuration. The black dots are the experimental data, and the solid curve is the theoretical fit.

Determination of the molecular weight of the polymer in DMF solution shows that the number-average molecular weight (M_n, 4336) and the weight-average molecular weight (M_w, 4437) are relatively larger, which indicated that the polymer is intact (or partly intact) in DMF solution.[20,21]

A preliminary study on the third-order NLO properties of **1** was carried out by the *Z*-scan method in a 1.0 × 10^{-5} M DMF solution. Figures 4 and 5 show typical *Z*-scan measurement of the cluster **1** in DMF solution. The nonlinear absorption component was evaluated under an open aperture. The filled squares represent the experimental data measured under this condition. It is clearly illustrated that absorption

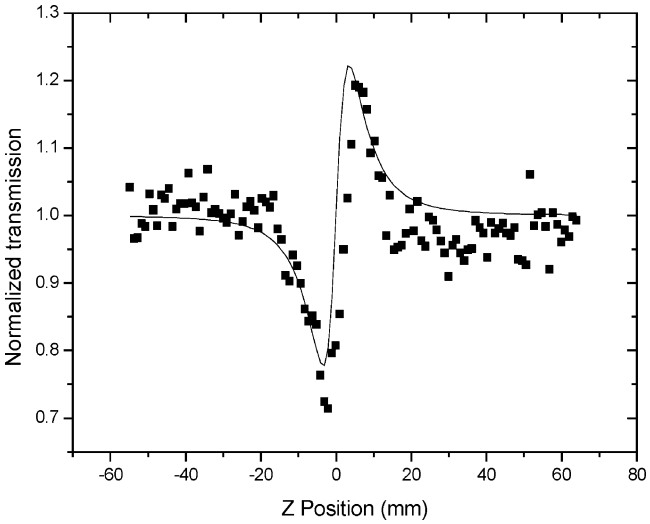

Figure 5. *Z*-scan data for **1** in 1.0 × 10^{-5} mol dm^{-3} DMF solution, obtained by dividing the normalized *Z*-scan measured under a closed aperture configuration by the normalized *Z*-scan data obtained under the open aperture configuration. The black dots are the experimental data, and the solid curve is the theoretical fit.

increases as the incident light irradiance rises. Since light transmittance (T) is a function of the sample's Z position (with respect to the focal point at $Z = 0$), the nonlinear absorption ($\alpha = \alpha_2(I_i)$) and linear absorption (α_0) can be well described by the classical eq 1, where α and α_0 are linear and effective third-order NLO absorptive coefficients, τ is the time, and L is the optical path. The solid lines in Figure 4 are the theoretical curves from the eq 1.

$$T(Z) = \frac{a_0}{\sqrt{\pi} a_2 I_i(Z)(1 - e^{-a_0 L})} \int_{-\infty}^{\infty} \times \ln\left[1 + a_2 I_i(Z) \frac{1 - e^{-a_0 L}}{a_0}\right] e^{-\tau^2} d\tau \quad (1)$$

A reasonably good fit between the experimental data (filled squares) and the theoretical curve was obtained, which in turn suggests that the experimentally observed nonlinear absorptivity is effectively a third-order process. The pattern of less discrepancy between the experimental data and theoretical curve indicates possible involvement of higher

(20) Hou, H. W.; Li, L. K.; Zhu, Y.; Fan, Y. T.; Qiao, Y. Q. *Inorg. Chem.* **2004**, *43*, 4767.
(21) Hou, H. W.; Meng, X. R.; Song, Y. L.; Fan, Y. T.; Zhu, Y.; Lu, H. J.; Du, C. X.; Shao, W. H. *Inorg. Chem.* **2002**, *41*, 4068.

order NLO processes. The effective nonlinear absorptive index α_2 is derived to be 1.044×10^{-9} mW^{-1} from the theoretical curve.

In addition to the nonlinear absorption, the compound also exhibits strong nonlinear refraction at 532 nm. The nonlinear refractive component of the compound was obtained by dividing the normalized *Z*-scan measured under a closed aperture configuration by the normalized *Z*-scan data obtained under the open aperture configuration (Figure 5). The valley and peak occur at equal distances from the focus. This result is consistent with the notion that observed optical nonlinearity has an effective third-order dependence on the incident electromagnetic field.[10] In addition, the valley−peak separation (ΔZ_{V-P}) and the difference between normalized transmittance values at valley and peak positions (ΔT_{V-P}) are found to fit to a set of eqs 2 and 3 derived for a third-order NLO process. An effective third-order nonlinear refractive index n_2 can be derived from the ΔT_{V-P} by using eq 3, where α_0 is the linear coefficient, L is the sample thickness, I is the peak irradiation intensity at focus, and λ is the wavelength of the laser. The refractive index n_2 was calculated to be 2.827×10^{-11} esu. The data show that the polymeric cluster has a positive sign for refractive nonlinearity, which indicates a self-focusing behavior.

$$\Delta Z_{V-P} = 1.72\pi\omega_0^2/\lambda \quad (2)$$

$$n_2^{\text{eff}} = \frac{\lambda\alpha_0}{0.812\pi I(1 - e^{-\alpha_0 L})}\Delta T_{V-P} \quad (3)$$

Those data are obviously better than those of the one-dimensional zigzag clusters $\{[MOS_3Cu_3(CN)(py)_3]\cdot 0.5C_6H_6\}_n$ (M = Mo or W).[22] From the α_2 and n_2 values, the effective third-order NLO susceptibility $\chi^{(3)}$ values of **1** can be calculated according to

$$\chi^{(3)} = \sqrt{\left|\frac{9 \times 10^8 \in_0 n_0^2 c^2}{4\pi\omega}\alpha_2\right|^2 + \left|\frac{cn_0^2}{80\pi}n_2\right|^2} \quad (4)$$

The $\chi^{(3)}$ value was calculated to be 4.13×10^{-12} esu. All these measured values were obtained with 1×10^{-5} mol dm^{-3} DMF solution of the title compound (limited by its solubility); a much larger value may be expected with more concentrated solutions provided the solubility can be increased.

Optical Limiting Effects. The combination of the self-focusing and nonlinear absorption makes the polymer an interesting candidate for optical limiting application. The optical limiting experiments show that the present cluster exhibits a better optical limiting capacity, which is demonstrated in Figure 6. Experiments with DMF solvents alone afforded no detectable OL effect. This indicates that the solvent contribution is negligible. At very low fluence they respond linearly to the incident light fluence obeying Beer's law. The light transmittance starts to deviate from Beer's law of the linear response when the input light fluence rises to 0.069 J cm^{-2}. The limiting threshold is defined as the incident fluence at which the solution transmittance falls to 50% of the linear transmittance. The value of the limiting threshold was measured as 0.53 J cm^{-2} from the optical limiting experimental data. Lower limiting threshold and saturation level provide greater safety margin for device protection. It is interesting to compare this new cluster with other well-known optical limiting materials for 7 ns pulsed radiation of 532 nm wavelength. Table 3 gives the limiting thresholds of cluster **1**, oligomeric clusters, polymeric clusters, and C_{60}. It is clear that the limiting performance of **1** in the DMF solution is three times better than that displayed in C_{60}. From the perspective of the OL application, the present cluster with polymeric 1D "chain" structure is comparable to (or slightly better than) the known good optical limiting materials, the one-dimensional helical cluster $\{[La(Me_2SO)_8][(\mu\text{-}WSe_4)_3Ag_3]\}_n$,[23] two-dimensional microporous polymer clusters $[MoS_4Cu_6I_4(py)_4]_n$[24] and $\{[NEt_4][Mo_2O_2S_6Cu_6I_3(4,4'\text{-bipy})_5]\cdot MeOH\cdot H_2O\}_n$,[4c] and three-dimensional microporous polymeric clusters $\{[Et_4N]_2[MS_4Cu_4(CN)_4]\}_n$.[25] The better optical limiting data for **1** than other 1−2D structures implies an overall balance effect on NLO of structure, heavy atom, and ligand impact. Although this threshold value from low concentration solution is not larger than that reported for 3D polymers, it is expected that higher threshold value could be attained if higher concentrations are attained and if the clusters could be deposited as thin films via CVD techniques. The successful synthesis of a series of coordination polymeric clusters by the polyiodide complex procedure illustrates the potential applicability of the method to the quick and facile preparation of novel NLO materials.

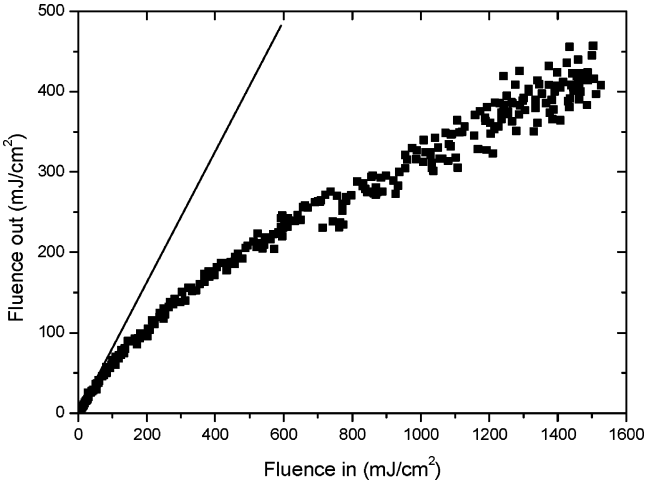

Figure 6. Optical limiting effect of $[(AgIC_{12}H_{10}N_4O_2)_6(KI)]_n$ (**1**) in a 1.0×10^{-5} mol dm^{-3} DMF solution.

(22) Hou, H. W.; Zheng, H. G.; Ang, H. G.; Fan, Y. T.; Low, M. K. M.; Zhu, Y.; Wang, W. L.; Xin, X. Q.; Ji, W.; Wong, W. T. *J. Chem. Soc., Dalton Trans.* **1999**, 2953.

(23) Zhang, Q. F.; Leung, W. H.; Xin, X. Q.; Fun. H. K. *Inorg. Chem.* **2000**, *39*, 417.

(24) Hou, H. W.; Fan, Y. T.; Du, C. X.; Zhu, Y.; Wang, W. L.; Xin, X. Q.; Low, M. K. M.; Ji, W.; Ang, H. G. *Chem. Commun.* **1999**, 647.

(25) Zhang, C.; Song, Y. L.; Xu, Y.; Fun, H. K.; Fang, G. Y.; Wang, Y. X.; Xin, X. Q. *J. Chem. Soc., Dalton Trans.* **2000**, 2823.

(26) Hou, H. W.; Xin, X. Q.; Liu, J.; Chen, M. Q.; Shi, S. *J. Chem. Soc., Dalton Trans.* **1994**, 3211.

(27) Ji, W.; Xie, W.; Tang, S. H.; Shi, S. *Mater. Chem. Phys.* **1996**, 4345.

Table 3. Limiting Thresholds of Available Oligomeric and Polymeric Clusters Measured at 532 nm with ns Laser Pulses

polymeric cluster	struct type	solvents	limiting threshold/J cm^{-2}	ref
C_{60}		toluene	1.6	2b
oligomeric clusters				
$[Et_4N]_4[Mo_2S_6Cu_6O_2Br_2I_4]$	twin nest-shaped	MeCN	2	26
$(n-Bu_4N)_4[Mo_8Cu_{12}O_8S_{24}]$	eicosanuclear	MeCN	0.7	27
polymeric clusters				
$\{[NEt_4][Mo_2O_2S_6Cu_6I_3(4,4'\text{-bipy})_5]\cdot MeOH\cdot H_2O\}_n$	2D microporous	DMF	0.4	4c
$[MoS_4Cu_6I_4(py)_4]_n$	2D microporous	DMSO	0.6	24
$\{[Et_4N]_2[MoS_4Cu_4(CN)_4]\}_n$	3D cross-framework	DMF	0.28	25
$\{[Et_4N]_2[WS_4Cu_4(CN)_4]\}_n$	3D cross-framework	DMF	0.15	25
$\{[Et_4N]_2[(\mu_4\text{-}WSe_4)Cu_4(CN)_4]\}_n$	3D cross-framework	DMF	0.2	23
$\{[La(Me_2SO)_8][(\mu\text{-}WSe_4)_3Ag_3]\}_n$	1D helical chain	DMF	0.7	23
$\{[AgI(inh)]_6(KI)\}_n$	1D polymeric	DMF	0.53	this work

Conclusion

By means of the "polyiodine complex method" we have successfully prepared a novel coordination polymeric cluster from the reaction of inh with AgI/KI in THF solution and clearly characterized the crystal structure. Polymer **1** represents to our knowledge the first example of coinstantaneous cation−anion-assisted supramolecular self-assembly with nanoscale inner cavities. Moreover, it is a very rare example of a $[Ag_6I_7]^-$ cluster with a very symmetric hexagram structure unit. On the basis of the *Z*-scan studies, its large optical limiting effect was also observed. The current work shows that constructing such molecules with above-mentioned advantages (high symmetry, extended array, heavy atoms, and σ-donor peripheral ligands) is perhaps a promising research direction in the search for better NLO materials. The synthesis and characterization of new types of homoiodometallic clusters with novel structural modes is expected to continue. Studies are also underway to probe the NLO mechanism of these cluster polymers and the stronger NLO effects and applicable OL properties.

Acknowledgment. This research was funded by the National Natural Science Foundation (Grant Nos. 20001006 and 20371042), the Excellent Young Teachers Program In Higher Education Institute, and the China Postdoctoral Science Foundation (Grant 2003033525).

Supporting Information Available: Crystallographic data for **1** in CIF format. This material is available free of charge via the Internet at http://pubs.acs.org.

IC0487023